Topological spin excitations on a rigid torus

V. L. Carvalho-Santos,[1,2] A. R. Moura,[1] W. A. Moura-Melo,[1,*] and A. R. Pereira[1]
[1]*Departamento de Física, Universidade Federal de Viçosa, 36570-000 Viçosa, Minas Gerais, Brazil*
[2]*Escola Agrotécnica Federal de Senhor do Bonfim, 48970-000 Senhor do Bonfim, Bahia, Brazil*
(Received 22 February 2008; revised manuscript received 19 March 2008; published 30 April 2008)

We study the Heisenberg model of classical spins lying on a toroidal support, whose internal and external radii are r and R, respectively. The isotropic regime is characterized by a fractional soliton solution. Whenever the torus size is very large, $R\to\infty$, its charge equals unity and the soliton effectively lies on an infinite cylinder. However, for $R=0$, the spherical geometry is recovered and we obtain that configuration and energy of a soliton lying on a sphere. Vortexlike configurations are also supported: in a ring torus ($R>r$), such excitations present no core where energy could blow up. At the limit $R\to\infty$, we are effectively describing it on an infinite cylinder, where the spins appear to be practically parallel to each other, which yields no net energy. On the other hand, in a horn torus ($R=r$), a singular core takes place, while for $R<r$ (spindle torus), two such singularities appear. If R is further diminished until it vanishesm we recover a vortex configuration on a sphere.

DOI: 10.1103/PhysRevB.77.134450 PACS number(s): 75.10.Hk

I. INTRODUCTION AND MOTIVATION

Geometrical and topological concepts and tools are important in many branches of natural sciences, particularly, in Physics. For instance, the idea of symmetry, which is intimately associated with geometry, is a keystone for studying a number of fundamental properties of several physical systems, e.g., the Noether theorem asserts a conserved quantity to each continuous symmetry of the associated action. Topology, in turn, is crucial for classifying and for giving stability to certain excitations, such as solitons (extending objects having finite energy) and vortices (presenting a nonvanishing vorticity around a given singular point or a topological obstruction). These and others have been observed in a number of systems, such as superconductors, superfluids, and magnetic materials, namely, vortexlike magnetization has been directly observed in nanomagnets.[1] On the other hand, the observed vortex-pair dissociation is the mechanism behind the topological phase transition.[2] Another kind of topological object emerges from Euclidian non-Abelian pure-field models in $(3+1)$ dimensions. They are called instantons, since they represent points in the Euclidian space-time. In this case, the relevant homotopy group is that associated with the mapping of the field space to the four-dimensional Euclidian one, so that $\pi_3(S^3\to S^3)=\mathbf{Z}$, for example, if the internal space is the QCD gauge group, $SU(3)$. Such excitations play an important role in this framework once the nonconservation of the flavor singlet axial current is proportional to the instanton charge.[3]

In turn, the toroidal geometry has recently received a considerable attention, for example, as tight traps for Bose-Einstein condensates, inside which the atoms develop a quasi-one-dimensional confined dynamics subject to periodic boundary conditions.[4] Ring-shaped carbon nanotubes have been shown to provide quasi-zero-dimensional systems whenever the rings are very small.[5,6] In addition, their topology also makes them possible field-effect transistors for technological applications[7] and a suitable control of their stable magnetization (e.g., those with a vortexlike profile) may be useful for applications in magnetoelectronic devices, namely, if an array of magnetic nanorings is concerned.[8] From a more fundamental point of view, it has been verified that whenever the Ising model is defined on a donut-shaped lattice, then, instead of a unique temperature, there appear two critical temperatures.[9] Even in Biology, the toroidal shape plays important roles: for instance, it has been observed that a large number of proteins involved in DNA metabolism adopt a ringlike shape, even though these proteins have quite distinct and unrelated functions in this mechanism. Why this geometry on topology is so abundant in this process and the reason why life evolution has selected it amongst many others remain a puzzle in specialized literature.[10]

Geometrically, a torus of genus 1 (one central hole) is a compact surface whose (Gaussian) curvature smoothly varies from $-1/r(R-r)$ to $+1/r(R+r)$ along its polar angle (see details below), so interpolating between the pseudospherical and spherical curvatures whenever $R>r$. From the topological point of view, the simplest genus-1 torus is obtained by the topological product of two circles, $T^1=S^1\wedge S^1$.[11] (In general, a genus-n torus is obtained in a similar way; for example, that of genus-2 is given by $T^2=T^1\wedge T^1$.) This confers that a nonsimple connectivity, say, closed loops holding on its central hole or the polar circumference, cannot be shrunk to a point (other nonsimply connected topologies are the ordinary circle and a disk with a hole, an annulus).

For studying classical spinlike textures, of solitonic and vortex kinds, on a torus, we first write down the continuum version of the Heisenberg (exchange) Hamiltonian in this geometry (Sec. II). Later, the nonlinear Euler–Lagrange equations are obtained and some particular cases are explicitly considered to describe the desired excitations. In addition, their profiles, energies, and other basic properties are discussed and compared to their counterparts from other surfaces. These tasks are performed in Sec. III, where solitonic-like solutions in the isotropic regime are described and, in Sec. IV, which is dedicated to vortexlike configurations, are studied within the planar rotator model (equivalently, the XY model, deals only with static properties). Finally, we and our paper by pointing out our conclusions and prospects for a forthcoming investigation in Sec. V.

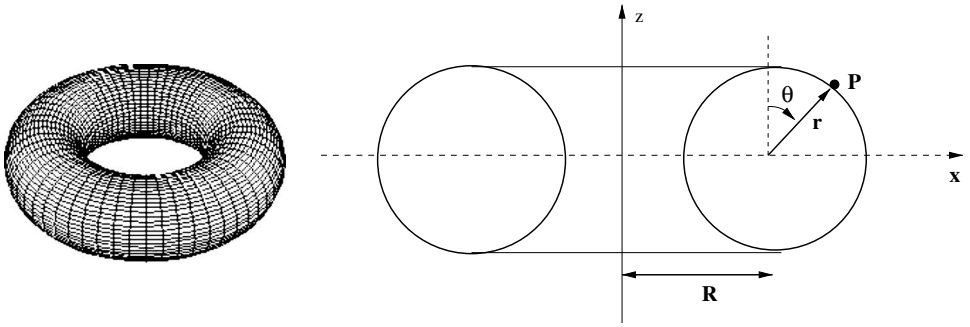

FIG. 1. Shape of an ordinary ring torus embedded in a three-dimensional space (left). Its cross section and the variables used throughout this work (right). The azimuthlike angle, ϕ, runs along the torus tube, z-constant planes, and is not shown in the cut.

II. CONTINUUM HEISENBERG MODEL ON THE TORUS

The anisotropic exchange Heisenberg model, for nearest-neighbor interacting spins on a two-dimensional lattice, is given by the Hamiltonian below:

$$H_{latt} = -J' \sum_{\langle i,j \rangle} \mathcal{H}_{i,j} = -J' \sum_{\langle i,j \rangle} [S_i^x S_j^x + S_i^y S_j^y + (1+\lambda) S_i^z S_j^z], \tag{1}$$

where J' denotes the coupling between neighboring spins and, according to $J'<0$ or $J'>0$, the Hamiltonian describes a ferro- or antiferromagnetic system, respectively. $\vec{S}_i = (S_i^x, S_i^y, S_i^z)$ is the spin operator at site i and the parameter λ accounts for the anisotropy interaction amongst spins: for $\lambda>0$, spins tend to align along the (internal) Z axis (easy-axis regime); for $\lambda=0$, one gets the isotropic case; for $-1<\lambda<0$, we have the easy-plane regime, while the $\lambda=-1$ case yields to the so-called XY model [or the planar rotator model (PRM) if we focus on a two-component spin, imposing $S_z \equiv 0$, so that $\vec{S}_{\mathrm{PRM}} = (S_x, S_y)$].

In the continuum approach of spatial and spin variables, valid at sufficiently large wavelength and low temperature, the Hamiltonian (1) may be written as $(J \equiv J'/2)$ follows:[12–14]

$$H_1 = J \iint \sum_{i,j=1}^{2} \sum_{a,b=1}^{3} g^{ij} h_{ab} (1 + \delta_{a3}\lambda) \left(\frac{\partial S^a}{\partial \eta_i}\right) \left(\frac{\partial S^b}{\partial \eta_j}\right) \sqrt{|g|}\, d\eta_1 d\eta_2$$

$$= J \int_\Omega \int (1 + \delta_{a3}\lambda)(\vec{D}S^a)^2 d\Omega, \tag{2}$$

where Ω is the surface with curvilinear coordinates η_1 and η_2, so that $d\Omega = \sqrt{|g|}\, d\eta_1 d\eta_2$, δ_{a3} is the Kronecker symbol, $\vec{D}$ is the covariant derivative, $\sqrt{|g|} = \sqrt{|\det[g_{ij}]|}$, and g_{ij} and h_{ab} are the elements of surface and spin space metrics, respectively (as usual, $g_{ij} g^{jk} = \delta_i^k$). Now, $\vec{S} = (S_x, S_y, S_z) \equiv (\sin\Theta\cos\Phi, \sin\Theta\sin\Phi, \cos\Theta)$ is the classical spin vector field valued on a unity sphere (internal space), so that $\Theta = \Theta(\eta_1, \eta_2)$ and $\Phi = \Phi(\eta_1, \eta_2)$. With this Cartesian parametrization for $\vec{S}$, we have $h_{ab} = \delta_{ab}$. The Hamiltonian (2) may also be viewed as an anisotropic nonlinear σ model, which lies on an arbitrary two-dimensional geometry, so that our considerations could have some relevance to other branches such as hydrodynamics, superfluidity, and superconductivity.

Our interest is to study the model above on the torus geometry, which is a smooth surface with varying curvature. The simplest torus is thought of as a surface having genus 1 (a single central hole) and, whenever embedded in three-dimensional space, it takes the shapes of a donut (see Fig. 1). The standard tori are classified in three distinct types concerning the relations between their internal r and external R radii. For $R>r$, we have a *ring torus* (donut shape, as shown in Fig. 1); if $R=r$, a *horn torus* is obtained, while for $R<r$, a *spindle torus* is described (the latter ones are depicted in Fig. 2).

Any ordinary torus may be parametrized in a simple way by some distinct coordinate systems, such as Cartesian[15] and peripolar[16] (θ, ϕ), so that

$$(R - \sqrt{x^2 + y^2})^2 + z^2 = r^2, \tag{3}$$

with the parametric equations

$$x = (R + r\sin\theta)\cos\phi, \quad y = (R + r\sin\theta)\sin\phi, \quad z = r\cos\theta, \tag{4}$$

where R and r are the rotating (external) and axial (internal) radii, respectively (see Fig. 1). In peripolar variables (θ, ϕ), the metric elements read

$$g_{\theta\theta} = r^2, \quad g_{\phi\phi} = (R + r\sin\theta)^2, \quad \text{and} \quad g_{\phi\theta} = g_{\theta\phi} = 0, \tag{5}$$

from which follows the Gaussian curvature:

$$K = \frac{\sin\theta}{r(R + r\sin\theta)}. \tag{6}$$

Note that K varies from $-1/r(R-r)$ at $\theta = 3\pi/2$ to $+1/r(R+r)$ at $\theta = \pi/2$. At $\theta = 0$ and π, the curvature vanishes. Indeed, as $R \to 0$, we get the sphere geometry once $K(R=0) = r^{-2}$, while for $R \to \infty$, we obtain a curvatureless infinite surface, like an infinite cylinder or an annulus. These points will be important later, whenever discussing the behavior of solitonic and vortex energies at these limits. Although we shall explicitly treat the case of a ring torus, $0<r<R$, our approach may be extended to the other standard tori, unless otherwise specified.

In this set of coordinates, the Hamiltonian (2) gets the form below $(\partial_\phi \equiv \frac{\partial}{\partial\phi}$ and $\partial_\theta \equiv \frac{\partial}{\partial\theta})$:

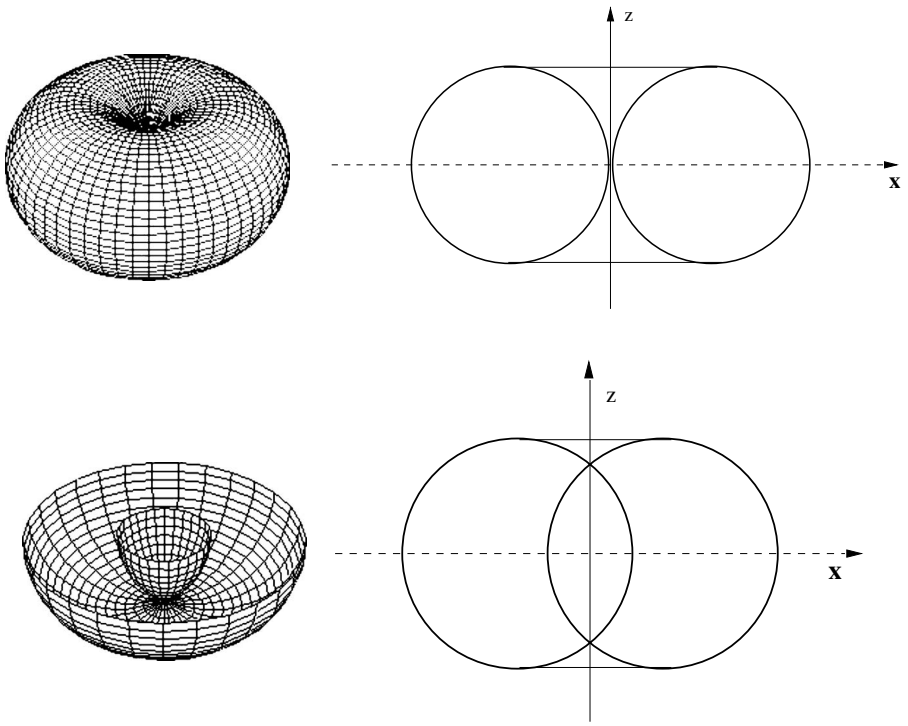

FIG. 2. Global and cross-section views of a horn (upper) and spindle tori (in this case, the torus was cut to improve global view). The parameters are those from Fig. 1. Note that in the cross sections, the horn and spindle tori have a single and a pair of self-intercepting points, respectively. Indeed, in the case of the spindle torus, such points correspond to two circumferences along which this surface crosses itself.

$$H = J\int_{-\pi}^{\pi}\int_{0}^{2\pi}\left\{\frac{r}{R+r\sin\theta}[(1+\lambda\sin^2\Theta)(\partial_\phi\Theta)^2+\sin^2\Theta(\partial_\phi\Phi)^2]+\frac{R+r\sin\theta}{r}[(1+\lambda\sin^2\Theta)(\partial_\theta\Theta)^2+\sin^2\Theta(\partial_\theta\Phi)^2]\right\}d\phi d\theta, \tag{7}$$

from which follow the (static) Euler–Lagrange equations for Θ and Φ, respectively:

$$\sin\Theta\cos\Theta\left\{\frac{r}{R+r\sin\theta}[\lambda(\partial_\phi\Theta)^2+(\partial_\phi\Phi)^2]+\frac{R+r\sin\theta}{r}[\lambda(\partial_\theta\Theta)^2+(\partial_\theta\Phi)^2]\right\}$$

$$=\cos\theta(1+\lambda\sin^2\Theta)(\partial_\theta\Theta)+\frac{R+r\sin\theta}{r}[(1+\lambda\sin^2\Theta)\partial_\theta^2\Theta+2\lambda\sin\Theta\cos\Theta(\partial_\theta\Theta)]$$

$$+\frac{r}{R+r\sin\theta}[(1+\lambda\sin^2\Theta)\partial_\phi^2\Theta+2\lambda\sin\Theta\cos\Theta(\partial_\phi\Theta)], \tag{8}$$

$$\cos\theta\sin^2\Theta\partial_\theta\Phi+\frac{R+r\sin\theta}{r}\partial_\theta(\sin^2\Theta\partial_\theta\Phi)+\frac{r}{R+r\sin\theta}\partial_\phi(\sin^2\Theta\partial_\phi\Phi)=0. \tag{9}$$

As expected, the general anisotropic regime of the Heisenberg model is described by nonlinear differential equations. Suitable nontrivial solutions can be obtained provided that some conditions are imposed, so that special solutions may be explicitly worked out. At this point, we should note that the equations above resemble in form those counterparts for the planar, spherical and pseudospherical surfaces. Indeed, whenever $R+r\sin\theta$ is identified with $\mathfrak{r}$, $\mathfrak{R}\sin\theta$, or $\varrho\tau$ while ϕ keeps its role as the azimuthlike angle, the expression above exactly recovers their planar, spherical, or pseudospherical analogs.[13,14] Above, $\mathfrak{r}=|\vec{\mathfrak{r}}|$ is the planar radial distance, $\mathfrak{R}$ is the sphere radius, while $\varrho\tau$ accounts for the distance measured along a pseudospherical geodesic, say, a hyperbole.

III. ISOTROPIC MODEL AND SOLITONIC SOLUTIONS

The simplest way to seek for possible solitonic solutions associated with the present model on a torus is by consider-

ing the isotropic regime, $\lambda=0$, and writing down the Hamiltonian (7), and its associated equations (8) and (9) in a more suitable coordinate system, which will allow us to get the sine-Gordon equation in a simpler way (further details may be found in Refs. 12 and 17). Such a coordinate system is parametrized by

$$x=\frac{a\sinh b\cos\varphi}{\cosh b-\sin\eta},\quad y=\frac{a\sinh b\sin\varphi}{\cosh b-\sin\eta},$$
$$z=\frac{a\cos\eta}{\cosh b-\sin\eta}, \tag{10}$$

where φ and η vary from 0 to 2π, while the constant parameters a and b are both real and positive, which impose that the above parametrization is valid only for the ring torus, $R>r$. In terms of r and R, we have

$$a=\sqrt{(R+r)(R-r)},\quad \cosh b=\frac{R}{r}, \tag{11}$$

which allow the interpretation of a and b as the *geometrical radius* and the *eccentric angle*, respectively.[17] Conversely, we have $R=a/\tanh b$ and $r=a/\sinh b$. In addition, it is easy to obtain the relations $\phi=\varphi$ and $\tan(\eta/2)=\sqrt{(R+r)/(R-r)}\tan(\theta/2)$. Therefore, in this set of coordinates, the Hamiltonian (7) describing toroidally symmetric solutions, $\Theta=\Theta(\varphi)$ and $\Phi=\Phi(\eta)$, gets the form

$$H=J\int_0^{2\pi}d\varphi\int_0^{2\pi}d\eta\left[\frac{(\partial_\varphi\Theta)^2}{\sinh b}+\sinh b\sin^2\Theta(\partial_\eta\Phi)^2\right], \tag{12}$$

while Eqs. (8) and (9) read

$$\sin\Theta\cos\Theta(\partial_\eta\Phi)^2=\sinh^{-2}b\,\partial_\varphi^2\Theta\quad\text{and}\quad\partial_\eta^2\Phi=0. \tag{13}$$

The latter equation has the simplest solution $\Phi(\eta)=\eta+\eta_0$, which, after substitution in the first one, gives us the sine-Gordon equation (with $\xi=\varphi\sinh b$) as follows:

$$\partial_\xi^2\Theta=\sin\Theta\cos\Theta, \tag{14}$$

whose simplest solution reads:[12,18]

$$\Theta(\varphi)=2\arctan(e^{\varphi\sinh b}), \tag{15}$$

with energy

$$E_{ring}=8\pi J\tanh(\pi\sinh b)=8\pi J\tanh\left(\pi\sqrt{\frac{R^2}{r^2}-1}\right)\leqslant 8\pi J, \tag{16}$$

which is in agreement with the saturated Bogomol'nyi inequality,[19] $E_{soliton}=8\pi J|Q|$, once, if we evaluate the solitonic charge, $Q=\frac{1}{4\pi}\int\sin\Theta d\Theta d\Phi$, for the solution above, we exactly obtain $Q_{\text{ring}}=\tanh(\pi\sinh b)$. Figure 3 shows how the solitonic charge behaves with the torus size, R. Namely, note that only when $R\to\infty$ ($\sinh b\to\infty$) does this charge equal unity. At this limit, the soliton agrees with its counterpart, which lies in an infinite cylinder and represents a complete mapping from the spin sphere to the target manifold (the torus), a π soliton, so corresponding to the first homotopy class of the second homotopy group of the mapping of the spin sphere to the (infinite) torus, say, $\pi_2(S^2\to T^1|_{R\to\infty})=\mathbf{Z}$. However, for finite R, such a mapping is incomplete and no homotopy arguments can be used for classifying solution (15) as a topological excitation. Indeed, in this case, we must take into account the topology of the geometrical support: although the genus prevents the complete mapping from the spin sphere onto the torus (so that the solution presents a fractional charge, $|Q|<1$), at the same time, it also ensures topological stability, in principle, preventing the fractional soliton from decaying against the ground state. In other words, now the soliton acquires a finite characteristic length, proportional to the genus size, which prevents its collapse and, consequently, its size from vanishing. Similar scenarios are provided by the annulus, the truncated cone,[20] and by the punctured pseudosphere.[13]

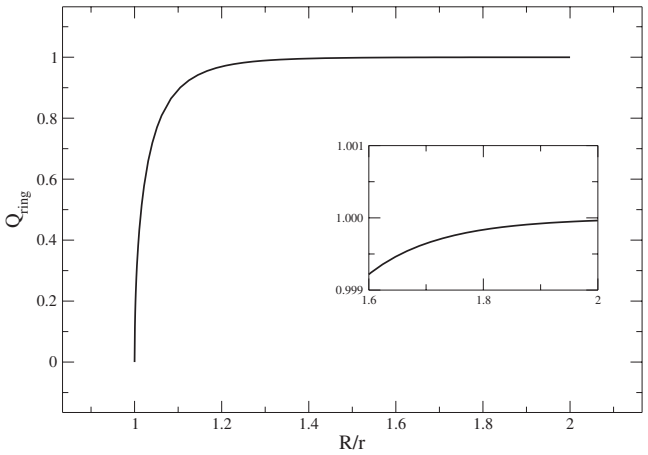

FIG. 3. How the solitonic charge associated with solution (15) behaves in the ring torus as a function of $R/r>1$. Although Q approaches unity very fast (e.g., for $R/r=2$, we obtain $Q_{R=2r}\approx 0.999\,95$; see inset), it should be stressed that only when $R\to\infty$ do we get $Q=1$.

Once the torus is the topological product of two circles, we may wonder whether another solitonic solution depending on the polar angle (θ or η), $\Theta(\theta)$, should not also appear in this framework. This is, indeed, the case. If we reconsider Hamiltonian (7) with the conditions $\lambda=0$, $\Theta=\Theta(\theta)$, and $\Phi=\Phi(\phi)$, we get

$$H_2=J\int_{-\pi}^{\pi}d\phi\int_0^{2\pi}d\theta\left[\left(\frac{r}{R+r\sin\theta}\right)\sin^2\Theta(\partial_\phi\Phi)^2+\left(\frac{R+r\sin\theta}{r}\right)(\partial_\theta\Theta)^2\right], \tag{17}$$

from which we obtain

$$\partial_\phi^2\Phi=0\quad\text{and}\quad\left(\frac{r}{R+r\sin\theta}\right)\sin\Theta\cos\Theta(\partial_\phi\Phi)^2=\cos\theta(\partial_\theta\Theta)+\left(\frac{R+r\sin\theta}{r}\right)(\partial_\theta^2\Theta). \tag{18}$$

The first equation is readily solved, giving $\Phi=\phi+\phi_0$, so that the latter one is simplified to

$$\left(\frac{r}{R+r\sin\theta}\right)\sin\Theta\cos\Theta$$
$$=\cos\theta(\partial_\theta\Theta)+\left(\frac{R+r\sin\theta}{r}\right)(\partial_\theta^2\Theta). \quad (19)$$

This expression is a generalized sine-Gordon equation, with nonconstant coefficients. In principle, the equation above admits solitonic solutions (possibly with fractional charge), but a closed and analytical solution is still lacking.[20] A further light into this issue may be shed if we take $R\to 0$ above. At this limit, the equation above gets the simple form

$$\sin\Theta\cos\Theta=\sin\theta\cos\theta(\partial_\theta\Theta)+\sin^2\theta(\partial_\theta^2\Theta), \quad (20)$$

which is easily solved by

$$\Theta(\theta)=\pm\theta, \quad (21)$$

which is precisely the simplest solution we have for the spherical geometry,[14,21] whose energy reads $E_{\text{sphere}}=8\pi J$, corresponding to the fundamental solitons with charges ± 1. Therefore, we have seen that solitonic solutions lying on a torus generally present (or are expected to) fractional charges. These charges equal unity only at specific limits: for $R\to\infty$, we effectively get a soliton on an infinite cylinder, while for $R\to 0$, the spherical counterpart is obtained.

IV. VORTEXLIKE SOLUTIONS ON THE TORUS

Geometrically, a vortex with a net winding number $\kappa\neq 0$ may be viewed as a set of spins rotating in a closed circuit around a core (whose center is a singular point) or a topological obstruction, which makes it impossible to change the configuration to a perfectly aligned state without tampering with spins at an arbitrary distance from the core. Thus, once a vortexlike configuration cannot be continuously deformed to the ground state, it acquires the status of a topologically stable excitation. Vortices have been intensively studied for decades in a number of physical systems, such as superfluids and superconductors, and they have been recently observed in several nanomagnets as remanent states of the net magnetization.[1] In addition, they have been proposed to take part (and even to be the key elements) in some magnetoelectronic mechanisms with potential applications to magnetic recording, processing, sensors, and so forth.[22]

When we model a vortex as a continuum of spins, we intend to describe only its outer region; once inside the core, the analytical treatment is expected to give only an estimate of its energy, shedding no light about its real structure and spins arrangement, which require numeric or simulation techniques. However, as we shall see, in the toroidal topology, a natural cutoff for the vortex is provided by the genus whenever $R-r>0$, so that, in a ring torus, the solution presents no core. On the other hand, in the case of a horn torus ($R=r$), a singular core takes place, while for $R<r$ (spindle torus), two singular points are verified. In both cases, the cores appear at the self-intercepting points (discussed earlier, see Fig. 2 and related text).

To achieve our purposes, we shall consider the planar rotator model, whose continuum Hamiltonian may be obtained from Eq. (7) with $\lambda=-1$ and $\Theta=\pi/2$ (once we are dealing with static solutions, our results apply equally well to the XY model), so that

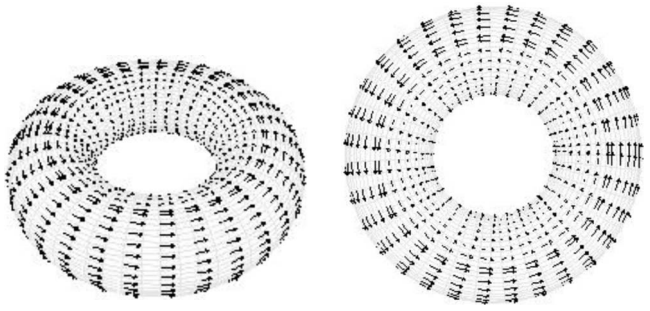

FIG. 4. Global (left) and top (right) views of a vortex with $\kappa=+1$ on the ring torus. The arrows represent the spin field, $\nabla\Phi$. The genus holds as a natural cutoff, preventing any core formation where energy could spuriously diverge.

$$H=J\int_0^{2\pi}\int_0^{2\pi}\left[\frac{r}{R+r\sin\theta}(\partial_\phi\Phi)^2+\frac{R+r\sin\theta}{r}(\partial_\theta\Phi)^2\right]d\phi d\theta. \quad (22)$$

Demanding Φ to be cylindrically symmetric, $\Phi=\Phi(\phi)$, the Hamiltonian above yields the following:

$$\partial_\phi^2\Phi=0\Rightarrow\Phi(\phi)=\kappa\phi+\phi_0, \quad (23)$$

where κ is the charge of the vortex, while ϕ_0 is a constant accounting for its global profile, which gives no contribution to its exchange energy. The charge (vorticity) is formally defined, in the continuum limit, as

$$\kappa=\frac{1}{2\pi}\oint_C(\vec{\nabla}\Phi)\cdot d\vec{l}, \quad (24)$$

where the integration is evaluated along a closed path C around the genus of the torus. By taking the solution above to the Hamiltonian (22), we obtain, for a ring torus ($R>r$),

$$E_{\text{v-ring}}=4\pi^2J\kappa^2\frac{r}{\sqrt{R^2-r^2}}, \quad (25)$$

from which we see that, distinctly from other cases (planar, conical, spherical, or pseudospherical geometries), the energy of a vortex in a ring torus does not present singularities, so that no cutoff needs to be introduced to prevent spurious divergences. The profile of a vortex with $\kappa=+1$ and $\phi_0=0$ is presented in Fig. 4. Note that its energy increases with r and decreases as R is raised. In addition, note that as $R\to\infty$, then $E_{\text{v-ring}}$ vanishes, which is expected since at this limit we effectively deal with the spins lying along the axial direction of an infinite cylinder, parallel to each other (in the ferromagnetic case). Thus, instead of a true vortex, we have the ground-state configuration in this flat geometry, whose normalized energy vanishes.

A similar analysis may be suitably employed for the remaining supports. However, in the case of a horn torus ($R=r>0$), Hamiltonian (22) diverges for the vortex solution

(23). This is not surprising since for this case the genus of the torus has been shrunk to a point (but it is not absent) where a singular core may be developed. Now, this spurious divergence must be bypassed by introducing a cutoff around the vortex core size, l_0. By doing that, the vortex energy on a horn torus may be easily evaluated to give

$$E_{\text{v-horn}} = 4\pi J\kappa^2 \cot(l_0/2r), \tag{26}$$

which depends only on the relative sizes of the core to the vortex, l_0/r. The singular core appears exactly where the horn torus is self-intercepting. This will also happen to the spindle torus, where a pair of singularities takes place, once this surface crosses itself at two distinct points (in variable θ), as follows.

If we insist in configurations like $\Phi=\Phi(\phi)$, we clearly realize that the energy density diverges at those two points where the spindle torus is self-intercepting, say, $R+r\sin\theta=0$. Integrating Hamiltonian (22) with solution (23), but keeping θ arbitrary, gives

$$\epsilon_{\text{spindle}} = 2\pi\kappa^2 J \frac{r}{\sqrt{r^2-R^2}} \ln\left(\frac{r-\sqrt{r^2-R^2}+R\tan(\theta/2)}{r+\sqrt{r^2-R^2}+R\tan(\theta/2)}\right). \tag{27}$$

To extract some finite and meaningful quantities, we must evaluate the result above over proper intervals. For that, we should introduce suitable cutoffs around those points where the energy density given by Eq. (22) blows up, say, $\theta_{\text{sing}}=\arcsin(-R/r)$ and $\pi-\arcsin(-R/r)$, and only later should we suitably evaluate $\epsilon_{\text{spindle}}$ in order to bypass the singularities. However, this task is very tedious and results in a very lengthy expression, which will be omitted here. The main feature is that the well-defined vortex energy clearly shows the appearance of two singular cores located at both θ_{sing}, which is given above. Another interesting issue is that whenever $R\to 0$, then an integration of the Hamiltonian (22) for solution (23) gives us exactly that result obtained in the spherical case,[14] namely, exhibiting the pair of cores at antipodal points. In summary, if we start off with a ring torus ($R>r$) where the vortex is coreless and decrease R, we eventually get a horn torus, where a core is formed. By decreasing R further, a spindle torus is obtained and the vortex now presents a pair of singular cores at the self-intercepting points. At the limit $R\to 0$, these cores are located at diametrically opposite positions and, effectively, we have a vortex lying on a sphere of radius r.

As previously discussed for the solitonic case, we could look for "vortexlike" solutions depending on the polar angle, say, $\Phi=\Phi(\theta)$. For this case, Hamiltonian (22) yields

$$\partial_\theta\Phi = \kappa' \frac{r}{R+r\sin\theta}, \tag{28}$$

while the topological charge is given by $k_\theta \equiv \frac{1}{2\pi}\oint(\nabla\Phi)\cdot d\vec{l}_\theta = \kappa' r/\sqrt{R^2-r^2}$ (so, valid only for the ring torus). Therefore, the solution of the equation above may be written as

$$\Phi(\theta) = 2\kappa_\theta \arctan\left(\frac{r+R\tan(\theta/2)}{\sqrt{R^2-r^2}}\right) + \theta_0, \tag{29}$$

whose energy is easily evaluated and give

$$E_{\theta\text{-ring}} = 4\pi^2\kappa_\theta^2 J \frac{\sqrt{R^2-r^2}}{r}, \tag{30}$$

which blows up as the ring torus becomes infinite, $R\to\infty$.

V. CONCLUSIONS AND PROSPECTS

We have studied the Heisenberg exchange model for classical spins defined on a toroidal geometry on topology. Solitonic- and vortex-type configurations were described in some detail, including their energy, profile, and behavior at some limiting cases of the torus size and geometry.

We first considered the isotropic regime. There, only for the ring torus ($R>r$) were solitonic solutions analytically obtained. These solutions appear to bear fractional charges, while their stability could be ensured, in principle, by the nontrivial topology of this torus, which is provided by the finite size of its central hole, $R-r>0$. As R increases, such a charge is raised but equals unity only for $R\to\infty$ (in practice, a soliton in an infinite cylinder). On the other hand, as $R\to 0$, a soliton lying on a sphere is described.

Now, by taking the XY regime, we have investigated vortexlike configurations in this support. In a ring torus, the vortex exhibits no core and its energy density is finite everywhere. Its net energy vanishes as $R\to\infty$, once the spins are now practically parallel to each other (the ferromagnetic ground state). If $R=r$ (horn torus), then the vortex develops a singular core at the self-intercepting point, while for $R<r$ (spindle torus), a pair of such cores appear, so that as $R\to 0$, they tend to be located at antipodal points and we recover the spherical case.

An interesting problem to be investigated is a small nanoring, say, with the geometry and topology of a ring torus. Actually, the expression *nanorings* frequently appears in nanomagnetic literature, including some possibilities for actual applications.[8] Such an object is generally fabricated by making a sufficiently large centered hole in a thin cylindrical nanodisk. Although it shares the torus topology, its geometry does not; once at the disk and hole borders, curvature abruptly changes. In addition, magnetostatic energies, which are very sensitive to the size and geometry of the magnet, are relevant in these cases, so that their evaluation in smoother supports seems to be more manageable, which justifies our prospect. Furthermore, our results could have some relevance for other branches where topological excitations and/or toroidal surfaces are concerned.

ACKNOWLEDGMENTS

The authors thank CNPq and Fapemig for partial financial support.

*winder@ufv.br

[1] T. Shinjo, T. Okuno, R. Hassdorf, K. Shigeto, and T. Ono, Science **289**, 930 (2000); J. Miltat and A. Thiaville, *ibid.* **298**, 555 (2002); A. Wachowiak, J. Wiebe, M. Bode, O. Pietzsch, M. Morgenstern, and R. Wiesendanger, *ibid.* **298**, 557 (2002).

[2] V. L. Berezinskii, Sov. Phys. JETP **32**, 493 (1970); **34**, 610 (1972); J. M. Kosterlitz and D. J. Thouless, J. Phys. C **6**, 1181 (1973).

[3] E. Witten, Nucl. Phys. B **156**, 269 (1979); G. Veneziano, *ibid.* **159**, 213 (1979); B. Allés, M. D'Elia, and A. Di Giacomo, *ibid.* **494**, 281 (1997).

[4] See, for example, F. M. H. Crompvoets, H. L. Bethlem, R. T. Jongma, and G. Meijer, Nature (London) **411**, 174 (2001); S. Gupta, K. W. Murch, K. L. Moore, T. P. Purdy, and D. M. Stamper-Kurn, Phys. Rev. Lett. **95**, 143201 (2005).

[5] For instance, see B. I. Dunlap, Phys. Rev. B **46**, 1933 (1992); J. Liu, H. Dai, J. H. Hafner, D. T. Colbert, R. E. Smalley, S. T. Tans, and C. Dekker, Nature (London) **385**, 780 (1997).

[6] S. Zhao, S. Zhang, M. Xia, E. Zhang, and X. Zuo, Phys. Lett. A **331**, 238 (2004).

[7] H. Watanabe, C. Manabe, T. Shigematsu, and M. Shimizu, Appl. Phys. Lett. **78**, 2928 (2001).

[8] See, for example, V. P. Kravchuk, D. D. Sheka, and Y. B. Gaididei, J. Magn. Magn. Mater. **310**, 116 (2007); P. Vavassori, A. Busato, A. Chiapatti, A. di Bona, S. Valeri, V. Metlushko, and B. Ilic, *ibid.* **316**, 944(E) (2007).

[9] I. Hasegawa, Y. Sakaniwaa, and H. Shima, J. Magn. Magn. Mater. **310**, 1401 (2007); Surf. Sci. **601**, 5232 (2007).

[10] A review is presented in M. M. Hingorani, and M. O' Donnel, Nat. Rev. Mol. Cell Biol. **1**, 22 (2000).

[11] M. Nakahara, *Geometry, Topology and Physics*, 2nd ed. (Taylor & Francis, London, 2003).

[12] A. Saxena, R. Dandoloff, and T. Lookman, Physica A **261**, 13 (1998).

[13] L. R. A. Belo, N. M. Oliveira-Neto, W. A. Moura-Melo, A. R. Pereira, and E. Ercolessi, Phys. Lett. A **365**, 463 (2007).

[14] G. S. Milagre and W. A. Moura-Melo, Phys. Lett. A **368**, 155 (2007).

[15] S. Wolfram, *Mathematica* (Cambridge University Press, Cambridge, England, 1999).

[16] Ou-Yang Zhong-can, Phys. Rev. A **41**, 4517 (1990).

[17] J. Benoit and R. Dandoloff, Phys. Lett. A **248**, 439 (1998).

[18] R. Rajaraman, *Solitons and Instantons: An Introduction to Quantum Field Theory* (North-Holland, Amsterdam, 1984).

[19] E. B. Bogomol'nyi, Sov. J. Nucl. Phys. **26**, 449 (1976).

[20] A. Saxena and R. Dandoloff, Phys. Rev. B **66**, 104414 (2002).

[21] S. Villain-Guillot, R. Dandoloff, A. Saxena, and A. R. Bishop, Phys. Rev. B **52** 6712 (1995).

[22] See, for example, M. Rahm, J. Stahl, W. Wegscheider, and D. Weiss, Appl. Phys. Lett. **85**, 1553 (2004); M. Rahm, J. Stahl, and D. Weiss, *ibid.* **87**, 182107 (2005); A. R. Pereira, A. R. Moura, W. A. Moura-Melo, D. F. Carneiro, S. A. Leonel, and P. Z. Coura, J. Appl. Phys. **101**, 034310 (2007).